Geomorphology 422 (2023) 108552

Contents lists available at ScienceDirect

Geomorphology

journal homepage: www.journals.elsevier.com/geomorphology

Vanishing evidence? On the longevity of geomorphic GLOF diagnostic features in the Tropical Andes

Adam Emmer *

Institute of Geography and Regional Science, University of Graz, Graz, Austria

ARTICLE INFO

Keywords:
Glacial lake outburst flood
GLOF
Geomorphic imprints, Andes
Cordillera Blanca

ABSTRACT

Trends in occurrence of glacial lake outburst floods (GLOFs) in space and time as well as frequency-magnitude relationships are typically derived from inventories of past GLOFs. Searching for geomorphic evidence (GLOF diagnostic features) in remote sensing images is a commonly used method for building GLOF inventories. In this study, I examine the longevity of geomorphic GLOF diagnostic features and thus the reliability of GLOF inventories that build on them. A set of 160 GLOFs documented from the Tropical Andes of Peru and Bolivia is analyzed, focusing on four GLOF diagnostic features: (i) breached dams; (ii) pre-GLOF water levels; (iii) outwash fans; (iv) impact areas. A total of 359 GLOF diagnostic features are identified and their evolution is analyzed from multi-decade remote sensing images, with special focus on GLOF diagnostic features that vanished in time. Building on these data, the expected longevity of GLOF diagnostic features is outlined, revealing long persistence of breached dams (>10^2 years), long persistence of pre-GLOF water levels (up to 10^2 years) and comparably more intense degradation and vanishing of outwash fans and impact areas. The main degradation processes of GLOF diagnostic features are identified, including the succession of vegetation, geomorphic reworking and anthropogenic activities. Further, the implications for building GLOF inventories are discussed, highlighting that vanishing geomorphic evidence of GLOF diagnostic features may lead to: (i) underestimated spatial extent of GLOF impact areas; and (ii) underestimated total numbers of GLOFs in GLOF inventories. Considering the number of major GLOFs as predictors of the number of minor GLOFs, an example of the Tropical Andes shows that the total number of GLOFs in the post-LIA period may be underestimated by up to 40 % (reference period 2011–2020).

1. Introduction

In recent decades, glacial lake outburst floods (GLOFs) became a phenomenon studied in glacierized regions all over the world (Emmer et al., 2022a). One of the branches of GLOF research focuses on building GLOF inventories for understanding their occurrence in space and time and frequency-magnitude relationships with clear utilization in disaster risk reduction efforts (e.g., Ikeda et al., 2016; Wang and Zhou, 2017; Motschmann et al., 2020; Haeberli and Drenkhan, 2022) as well as climate change attribution studies (Harrison et al., 2018). A number of updated GLOF inventories has been published, focusing on High Mountain Asia (Nie et al., 2018; Veh et al., 2019; Zheng et al., 2021), Iceland and Greenland (Carrivick and Tweed, 2019), Tropical Andes (Bat'ka et al., 2020; Emmer et al., 2022b) as well as Patagonian Andes (Jacquet et al., 2017). Those regional GLOF inventories fuelled a recent global inventory compiled by Veh et al. (2022), containing >2800 GLOFs globally, far exceeding previous attempts (Vilímek et al., 2014; Carrivick and Tweed, 2016).

Building GLOF inventories is a challenging task that requires the integration of various data sources (e.g., Emmer et al., 2016). Typically, a GLOF inventory exploits existing scientific literature (journal papers, books) and documentary data sources (e.g., archival research reports, disaster risk management technical reports, newspaper articles, chronicles; e.g., Emmer (2017); Carrivick and Tweed (2019)), in combination with manual or semi-automatic analysis of remote sensing images with field validation (e.g., Veh et al., 2018; Bat'ka et al., 2020), discharge gauge analysis (Carrivick et al., 2017) or sedimentologic analysis (Vandekerkhove et al., 2021; Piret et al., 2022). While comprehensive documentary as well as discharge data are only available for a few GLOF regions (e.g., Alps (Richard and Gay, 2004), Iceland (Carrivick and Tweed, 2019), Alaska (Abdel-Fattah et al., 2021)), sedimentologic analyses are demanding and traditionally rather used for exploring the

* Corresponding author at: Institute of Geography and Regional Science, University of Graz, Heinrichstraße 36, 8010 Graz, Austria.
E-mail addresses: adam.emmer@uni-graz.at, aemmer@seznam.cz.

https://doi.org/10.1016/j.geomorph.2022.108552
Received 22 September 2022; Received in revised form 12 November 2022; Accepted 1 December 2022
Available online 7 December 2022

occurrence of GLOFs on longer (e.g., Holocene) timescales (Rothe et al., 2019; Monegato et al., 2020). As such, the analysis of remote sensing images is the most frequently used approach employed in building GLOF inventories nowadays.

However, relying on the analysis of remote sensing images is associated with a number of limitations, despite the recent improvements in resolution and availability of various products (Kirschbaum et al., 2019; Taylor et al., 2021). First, the period covered by broadly available remote sensing images is relatively short (typically not going before 1980s in remote mountain regions), limiting the understanding of the wider temporal context of low frequency events such as GLOFs. Second, the spatial as well as temporal resolution of remote sensing data has historically been relatively coarse, favoring only major events to be identified and limiting precise dating of their occurrence. Third, the evidence of GLOFs is presumably preserved in the landscape for only limited time period and may be a subject of vanishing.

While the first and second points are not in the scope of this study, I focus on examining how long the geomorphic evidence of GLOFs (GLOF diagnostic features) is identifiable in the landscape (i.e., what is the longevity of GLOF diagnostic features). Building on the example of Topical Andes (Fig. 1) and recent inventory of 160 GLOFs that occurred in this region since the Little Ice Age (Emmer et al., 2022b), this study is the first attempt to quantify the longevity and expected longevity of geomorphic GLOF diagnostic features. The guiding questions of this study are: (i) Which GLOF diagnostic features are associated with GLOFs of different magnitudes and lake dam types?; (ii) How long do geomorphic GLOF diagnostic features persist in the landscape?; (iii) What are the processes behind the evolution (degradation) of developed GLOF diagnostic features?; (iv) What are the implications for existing GLOF inventories?

2. Data and methods

2.1. Defining and identifying geomorphic GLOF diagnostic features

Glacial lake outburst floods are associated with substantial geomorphic imprints that vary in nature, form as well as scale (Emmer, 2017; Jacquet et al., 2017; Maurer et al., 2020; Tomczyk et al., 2020)

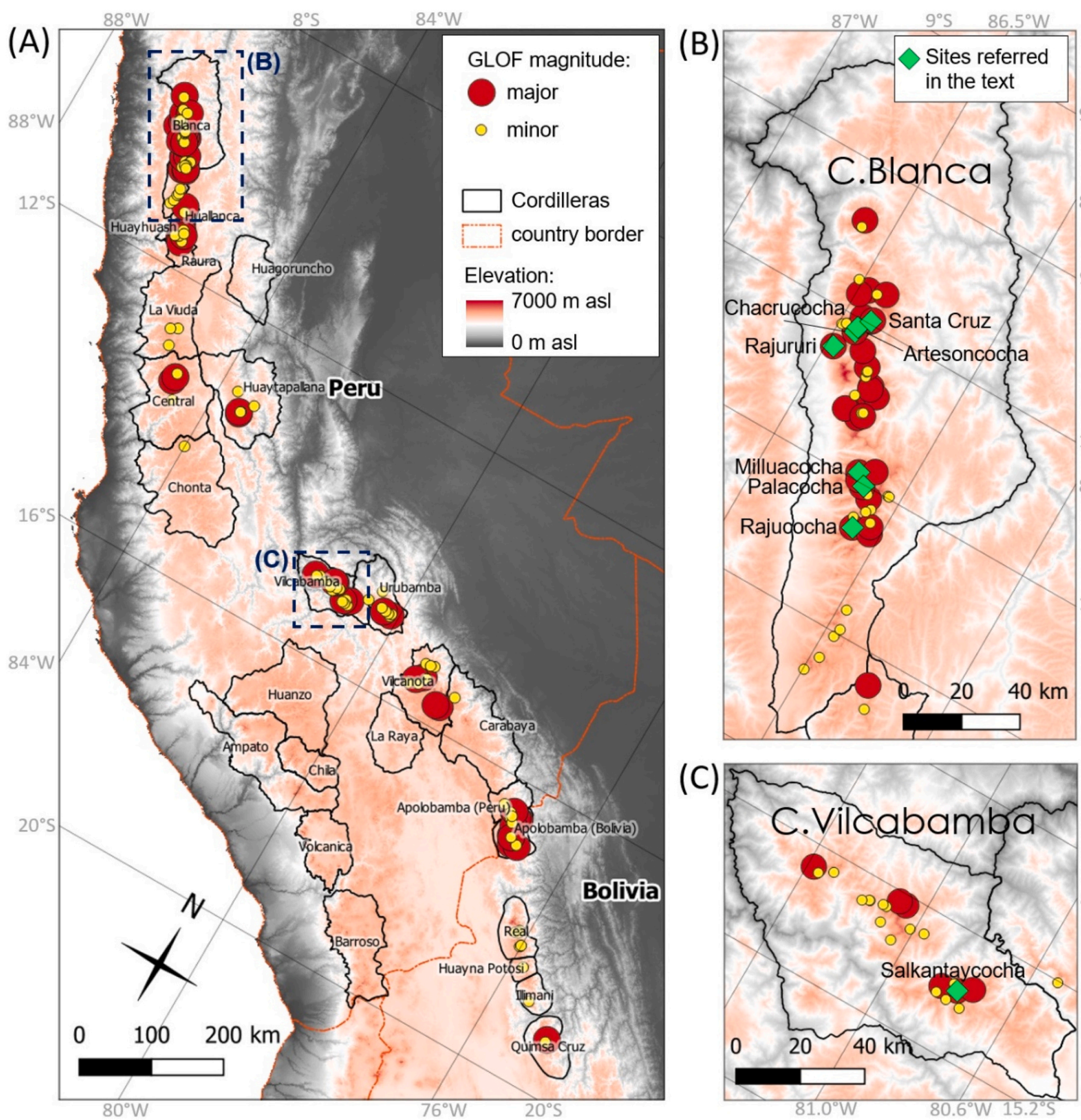

Fig. 1. The location of analyzed GLOFs and the sites referred in the text. Data: Emmer et al., 2022b (GLOF location and magnitude), USGS (GTOPO30 DEM), INAIGEM, 2018 (borders of individual Cordilleras).

and assumably also longevity. Four types of geomorphic GLOF diagnostic features are in the spotlight of this study. These are: (i) breached dam (Fig. 2A); (ii) evidence of pre-GLOF water level (Fig. 2B); (iii) outwash fan (Fig. 2A); (iv) impact area further downstream (Fig. 2C). Those are GLOF geomorphic features typically associated with GLOFs in the area of the Tropical Andes (Emmer, 2017; Bat'ka et al., 2020; Emmer et al., 2022b).

While a number of (semi-)automated approaches have been developed to monitor lake areas (e.g., Wang et al., 2020; Field et al., 2021) and to identify GLOF impact areas (Veh et al., 2018) with the use of medium-resolution multispectral images, these couldn't be applied in this work for two main reasons. First, remote sensing images of different origin, quality and resolution (see Section 2.3) are integrated in this work, substantially reducing meaningful applicability of (semi-)automated approaches. Second, these approaches can only be successfully employed if a pre-GLOF image is available (change detection), which would reduce the number of analyzable GLOFs considerably (see Section 2.2). Therefore, the identification of four studied types of GLOF diagnostic features is done by visual interpretation of optical remote sensing images, despite this procedure bears certain subjective component. The whole analysis has been done by a single person, ensuring the interpretation consistency. The visual interpretation of remote sensing images has been validated during repeated field visits in selected valleys in the Peruvian Cordillera Blanca, Cordillera Huayhuash and Cordillera Vilcabamba (10 months in total in between 2012 and 2022).

2.2. A set of examined GLOFs

Geomorphic imprints of GLOFs which are listed in the GLOF inventory of Peru and Bolivia prepared by Emmer et al. (2022b) are analyzed in this study. The inventory includes details about the total of 160 GLOFs that occurred from 151 lakes, while different lake dam types (moraine-dammed, bedrock-dammed, combined dams, ice-dammed) and GLOF mechanisms (dam breach, dam overtopping, piping) are represented (Fig. 1). Each GLOF in the inventory is described by a number of qualitative and quantitative characteristics and the reader is referred to the original study of Emmer et al. (2022b) for more details. The characteristics that are used in this study include: (i) the location of source lake (longitude and latitude); (ii) GLOF magnitude (major or minor); (iii) the timing of GLOF occurrence. GLOF magnitude was assigned by Emmer et al. (2022b) based on the reach of the flood (geomorphological imprints traceable >1 km from the source lake indicate major GLOF). At the same time, all GLOFs mentioned in documentary data sources are considered major events.

While lake location and GLOF magnitude are conclusively assigned to each GLOF in the inventory, the timing is only known for a subset of 89 GLOFs (56 %). All these GLOFs occurred in the post-Little Ice Age (post-LIA) period (i.e., palaeo-GLOFs are not a subject of this work). The main phase of the LIA is dated to culminate from mid-17th to early 18th Century in the Tropical Andes, with occasional regional re-advances later (Jomelli et al., 2008; Rabatel et al., 2013). The list of 89 GLOFs with known timing includes GLOFs with known exact year of occurrence (n = 69, i.e., 43 % of all) and GLOFs with the year of occurrence calculated from the closest pre-GLOF image and post-GLOF image (e.g., GLOF which occurred between 1962 and 1970 aerial image is considered to happen in 1966 in the analysis). This calculation has been used for 20 GLOFs (13 %).

Only open time interval is known for remaining 71 GLOFs (typically referring to the occurrence before the first available image, for example before 1948). Based on the location of the vast majority of GLOF-producing lakes within the LIA limits, not dated GLOFs are also assumed to occur in the post-LIA period (Emmer et al., 2022b). GLOFs with known year of occurrence (dated GLOFs) and GLOFs with unknown year of occurrence (not dated GLOFs) are treated differently in the

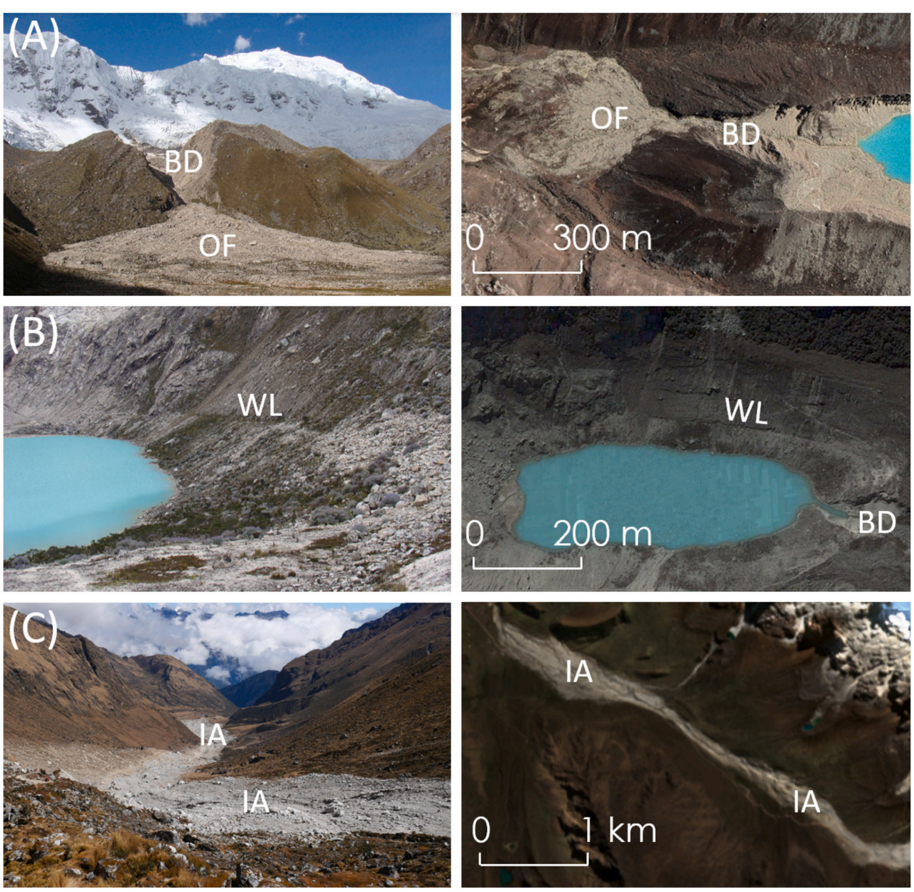

Fig. 2. Examples of different types of studied GLOF diagnostic features as seen from the ground and from the space. Part (A) shows the breached dam (BD) and outwash fan (OF) of the Lake Milluacocha, C. Blanca, Peru; shown diagnostic features are associated with the 1952 GLOF (satellite image: CNES / Airbus, 9th August 2021, available from Google Earth Pro collection); Part (B) shows well-preserved evidence of the pre-GLOF water level (WL) associated with the 1951 GLOF from the Lake Artesoncocha, C. Blanca, Peru (satellite image: Maxar technologies, 8th September 2003, available from Google Earth Pro collection); part (C) shows part of the impact area of the 2020 GLOF from the Lake Salkantaycocha (see also Vilca et al., 2021), C. Vilcabamba, Peru (satellite image: Sentinel-2, 16th July 2022, available from Sentinelhub EO browser collection).

analysis. The age of existing GLOF diagnostic features and the longevity of vanished GLOF diagnostic features are calculated for dated GLOFs while the minimum age of existing or vanished GLOF diagnostic features is calculated for not dated GLOFs (see Section 2.4 for details).

2.3. Remote sensing data

Remotely sensed optical images of various origin, spatial and temporal coverage and resolution were integrated in this study in order to shed light on the longevity of GLOF diagnostic features (see Table 1). These include aerial images and medium to very high-resolution satellite images. Considering the aim and scope of this study, the integration of various data sources is preferred over being ultimately consistent in terms of data used (consistent in temporal coverage and spatial resolution in different parts of the study area).

2.4. Workflow and the calculation of longevity, age and minimum age of GLOF diagnostic features

The workflow of this study has three consecutive steps which are depicted in Fig. 3. In the first step, developed GLOF diagnostic features were searched for each GLOF in the inventory (see Section 2.2). For this purpose, the first available post-GLOF images were used. The outcome of this search was a list of developed GLOF diagnostic features. In the second step, GLOF diagnostic features identified in the first step were sought in the most recent available images.

GLOF diagnostic features found in the first as well as last image formed a list of existing GLOF diagnostic features. The **age of existing GLOF diagnostic features** was calculated as the difference between the date of the last image and GLOF date, if known (for instance, the age of a breached dam associated with the 1941 GLOF, which is visible on 2021 image, is 80 years). In case of not dated GLOF, the **minimum age of existing GLOF diagnostic feature** was calculated as the difference between the date of the last image and the utmost GLOF date (for instance, the minimum age of a breached dam associated with the GLOF that occurred before 1948, which is visible on 2021 image, is 73 years).

GLOF diagnostic features that vanished in between the first post-GLOF image and the last image formed a list of vanished GLOF diagnostic features. In the third step, all GLOF diagnostic features from this list have been sought in multitemporal images in order to specify when they vanished. If the vanished diagnostic feature was associated with dated GLOF, **the longevity** was calculated as the difference between the date of the first image where a vanished GLOF diagnostic feature is not identifiable anymore and the GLOF date (for instance, the longevity of impact area associated with the 1959 GLOF, that vanished in between 1970 and 1985 image, is 26 years). In case of a not dated GLOF, the **minimum age of vanished GLOF diagnostic feature** was calculated as the difference between the first image where vanished GLOF diagnostic feature is not identifiable anymore and the utmost GLOF date (for instance, the minimum age of a breached dam associated with the GLOF that occurred before 1948, which vanished between 1962 and 1970 image, is 22 years).

2.5. Degradation processes of geomorphic GLOF diagnostic features

Based on the analysis of the evolution of GLOF diagnostic features (see Section 2.4), common degradation processes were identified and described in Section 3.3, based on the visual interpretation of multi-temporal optical remote sensing images. Each GLOF diagnostic feature from the list of developed GLOF diagnostic features was assigned dominant degradation process (if any) in order to reveal which processes are effective agents for individual types of studied GLOF diagnostic features. Finally, the effectiveness of degradation processes in vanishing GLOF diagnostic features is outlined.

3. Results

3.1. Developed GLOF diagnostic features

Out of the 160 analyzed GLOFs, 156 GLOFs developed one or more diagnostic features (Fig. 4) identifiable from post-GLOF remote sensing images. A total of 359 individual GLOF diagnostic features were observed and further analyzed. The most frequently occurring GLOF diagnostic features are outwash fans found in 128 (80 %) cases, followed by impact areas found in 114 (71 %) cases. Breached dams were observed in 80 (50 %) cases and the evidence of pre-GLOF water level was found in 37 (23 %) cases. The most common combination of two GLOF diagnostic features were outwash fan + impact area (43 cases; i.e., 27 %), while the most frequent combination of three GLOF diagnostic features were breached dam + outwash fan + impact area (30 cases; i.e., 19 %). All four studied GLOF diagnostic features were observed in 16 (10 %) cases. Three or four GLOF diagnostic feature were typically developed when the GLOF originated from moraine-dammed lake while GLOFs originating from bedrock-dammed lakes are typically only associated with outwash fans and impact areas (see Section 4.2). No GLOF diagnostic features were observed in 4 cases. Those are GLOFs mentioned in documentary data sources which exhibited no geomorphic GLOF diagnostic features in the post-GLOF remote sensing images. This is either because GLOF diagnostic features were not developed (all 4 GLOF occurred before the first available image) or because they vanished before the first image was taken.

Fig. 5 shows a comparison of GLOF diagnostic features associated with major GLOFs (n = 71) and minor GLOFs (n = 89). More than three out of four major GLOFs (76 %) developed outwash fans together with impact areas (including combinations with other two studied GLOF diagnostic features) while these two (+combinations) developed in less than half of minor GLOFs (48 %). More than a quarter of all minor GLOFs (27 %) developed only one GLOF diagnostic feature while less than one in eight major GLOFs (12 %) is characterized by only one GLOF diagnostic feature. On the other hand, the four GLOFs which developed no diagnostic feature (none were found in the available post-GLOF images) are classified as major events. Three GLOF diagnostic features were developed in 40 % of major GLOFs and 21 % minor GLOFs. All four GLOF diagnostic features were evident in 15 % of major and 6 % of minor GLOFs.

Table 1
RS data employed in this work.

Data	Temporal resolution	Temporal coverage	Spatial resolution	Spatial coverage	Availability
Google Earth Pro collection	Irregular (months to years)[a]	2002–2009 to present[a]	2 m to submetric[a]	Whole study area	Desktop version available from: https://www.google.com/intl/cs/earth/versions/
Landsat images	8 days	1982–2022	15 m to 30 m (visible spectra)	Whole study area	Available online from: https://landsatlook.usgs.gov
Sentinel 2 images	2 to 4 days	2015 - present	15 m (visible spectra)	Whole study area	Available online from: https://apps.sentinel-hub.com/eo-browser/
Aerial images	NA	1948, 1962, 1970	2 m	Cordillera Blanca	Original aerial images are available in the archive of the Autoridad Nacional del Agua, Huaraz, Peru

[a] The resolution as well as the temporal coverage of images in the Google Earth Pro collection vary across the study area.

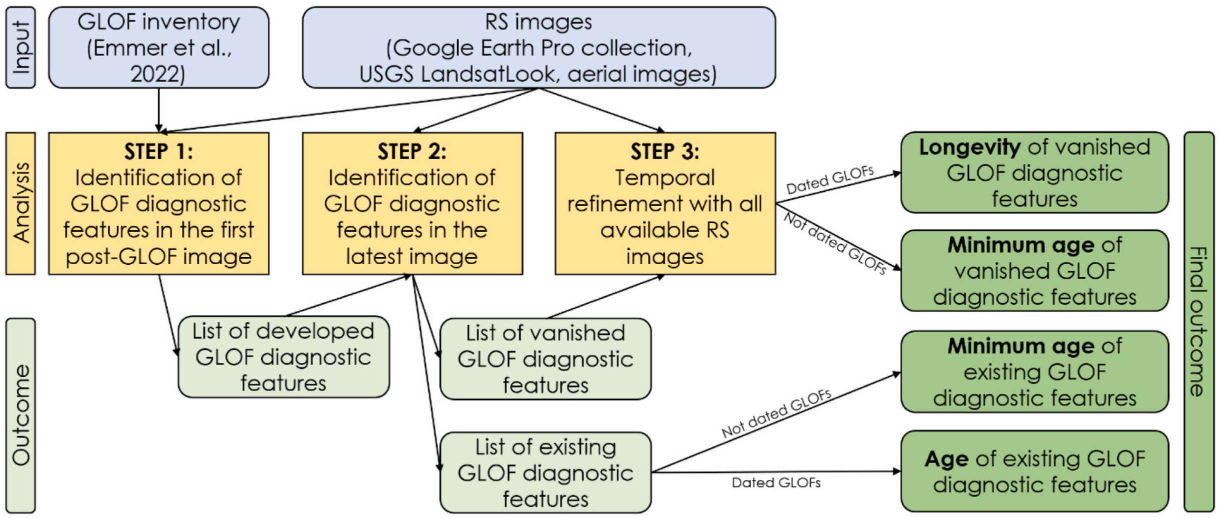

Fig. 3. Schematized workflow of deriving longevity, age and minimum age of GLOF diagnostic features. Input data, steps of the analysis, intermediate outcomes and final outcomes are shown.

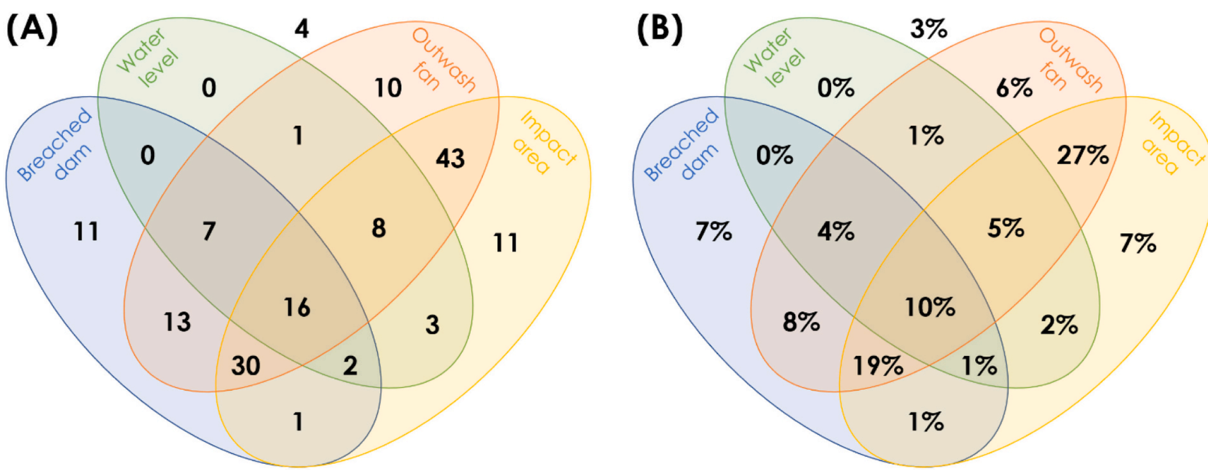

Fig. 4. An overview of developed GLOF diagnostic features and their combinations (based on the first available post-GLOF images) of 160 analyzed GLOFs. (A) shows absolute numbers. Each number in the graph represents the number of GLOFs which developed given combination of GLOF diagnostic features, 4 GLOFs which developed no diagnostic features are displayed outside the Venn diagram. (B) shows the share of GLOFs with given combinations of GLOF diagnostic features (rounded to integers).

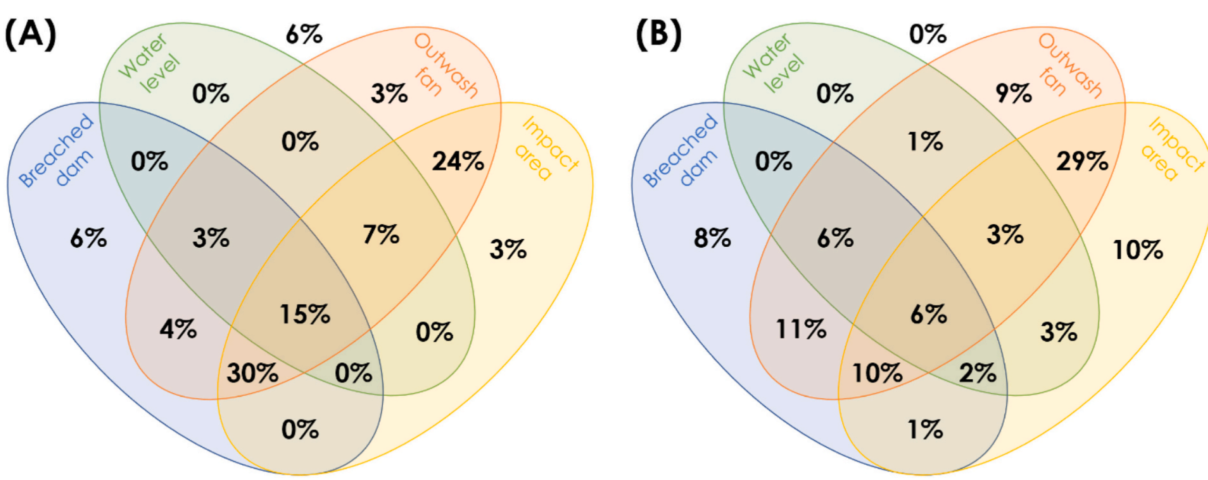

Fig. 5. The share of GLOFs with given combinations of GLOF diagnostic features associated with 71 major GLOFs (A) and 89 minor GLOFs (B). All values are rounded to integers.

3.2. Longevity, age and minimum age of GLOF diagnostic features

The results presented in Fig. 6 are structured in two categories. Part (A) shows the longevity of vanished GLOF diagnostic features, i.e., a period between a dated GLOF and the first image where the GLOF diagnostic feature is not identifiable anymore. A total of 58 data points is generated for this category, most of which relate to impact areas (n = 37 i.e., 32.5 % of all developed impact areas) and outwash fans (n = 16, i.e., 12.5 % of all developed outwash fans). The interquartile range of the longevity of these diagnostic features is 10–44 years, respectively 14–39 years, with median longevity being 18 and 25 years, respectively. However, substantial differences are observed when GLOF magnitude (major or minor) is taken into consideration. Maximum, quartile as well as minimum longevity is higher for major GLOFs for both diagnostic features. This difference is statistically significant for impact areas ($p < 0.01$; based on the two sample F-Test for variances and two sample *t*-test for means). Only two data points (15 and 121 years) were derived for breached dams and three data points (3, 6 and 11 years) for pre-GLOF water levels, indicating that their persistence is beyond the period of analyzed remote sensing images (1948–2021).

Part (B) shows the age of existing GLOF diagnostic features of dated GLOFs (196 data points). The age of existing breached dams (27 data points) varies from 2 to 120 years, with interquartile range 23–71 years and median age of 55 years. Only one data point is available for existing breached dam associated with a minor GLOF, corroborating that dam breaches are rather associated with major GLOFs. The age of existing pre-GLOF water levels varies from 0 to 89 years (17 data points), with interquartile range 2–55 years and median age of 10 years. The age of pre-GLOF water levels associated with major GLOFs (1 to 89 years, median age 29 years) and minor GLOFs (0 to 10 years, median age 4 years). The interquartile range of the age as well as median age of existing outwash fans (75 data points) and impact areas (77 data points) is in both cases smaller compared to the vanished outwash fans and impact areas (compare Fig. 6A and Fig. 6B). A statistically significant difference ($p < 0.01$; based on the two sample F-Test for variances and two sample t-test for means) is observed between the age of GLOF diagnostic features associated with minor and major GLOFs for pre-GLOF water levels, outwash fans and impact areas.

The data on minimum age of existing GLOF diagnostic features derived from not dated GLOFs (163 data points) indicates that the maximum minimum age of all types of GLOF diagnostic feature can demonstrably exceed 80 years. Those are GLOF diagnostic features associated with GLOFs which occurred before the first set of aerial images in 1948. However, these are extreme values for all GLOF diagnostic features with the exception of breached dams. The median value of minimum ages of diagnostic features associated with not dated GLOFs varies between 25 and 37 years and strongly reflects on the date of the first available images throughout the study area. The utilization of the minimum age is, therefore, only limited and observations are informative rather than conclusive.

Most importantly, the analysis of development of GLOF diagnostic features in time reveals that: (i) only few breached dams vanished during the analyzed period, suggesting their generally long persistence (longevity); (ii) pre-GLOF water levels exhibit long persistence but also less frequent occurrence (less than one in four GLOF); (iii) outwash fans and impact areas are GLOF diagnostic features which experienced the most intense degradation; (iv) the longevity of diagnostic features associated with major GLOFs is higher compared to diagnostic features associated with minor GLOFs. Synthesizing these observations with quantitative data from the analysis of the longevity and the age of existing GLOF diagnostic features allowed to outline the expected longevity of GLOF diagnostic features (Table 2). The expected longevity of breached dams of major GLOFs is expected to exceed 10^2 years, while the expected longevity of other diagnostic features associated with major GLOFs is 10^1 to 10^2 years. In the case of minor GLOFs, the expected longevity of breached dams is 10^1 to 10^2 years, while the expected longevity of other diagnostic features is <50 years.

Table 2
The synthesis of expected longevity of GLOF diagnostic features for minor and major GLOFs.

GLOF diagnostic feature	Major GLOFs	Minor GLOFs
Breached dam	$>10^2$ years	10^1–10^2 years
Pre-GLOF water level	10^0–10^2 years	<50 years
Outwash fan	10^1–10^2 years	<50 years
GLOF impact area	10^1–10^2 years	<50 years

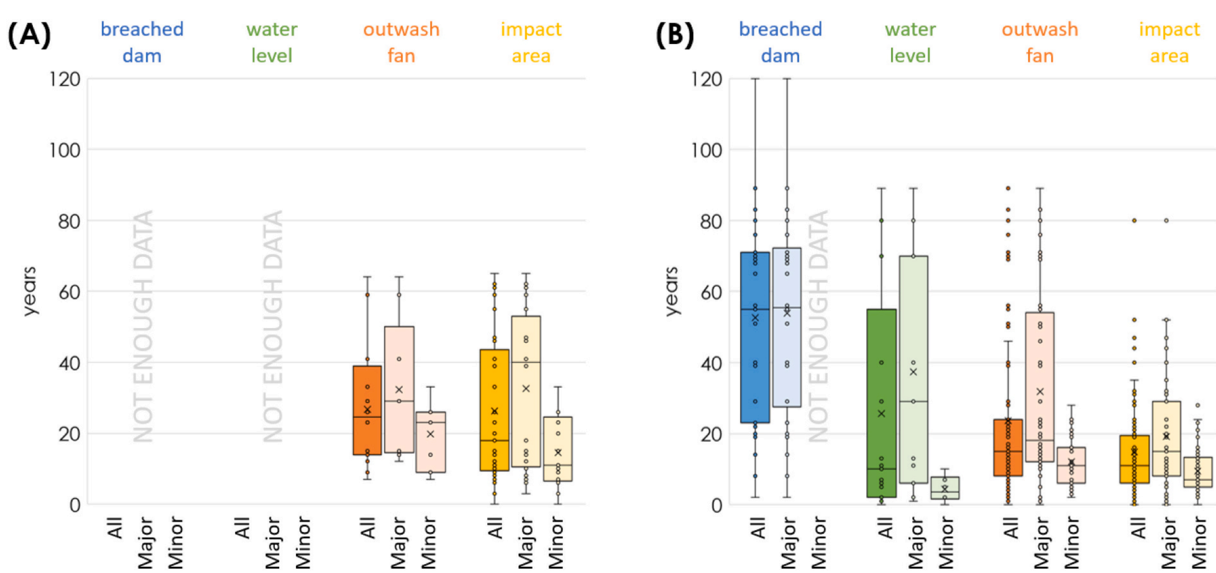

Fig. 6. The longevity of vanished GLOF diagnostic features (A) and the age of existing GLOF diagnostic features of dated GLOFs (B). Separate boxplots for all, major and minor GLOFs are shown. The boxes show a range between the 1st and the 3rd quartile (interquartile range, IQR) and the median (2nd quartile), individual data points are displayed as circles, while (virtual) mean value is displayed as x. Vertical lines show data points within the range up to +/− 1.5*IQR from the box.

3.3. Degradation processes of geomorphic GLOF diagnostic features in time

3.3.1. Observed degradation processes

The analysis of the development of geomorphic GLOF diagnostic features in time revealed three main degradation processes. These are: (i) succession of vegetation; (ii) geomorphic reworking; and (iii) anthropogenic activities. The succession of vegetation (grass, shrubs, trees) was observed especially on diagnostic features with flatter surfaces (outwash fans, impact areas and exposed, previously submerged areas). The location of GLOF diagnostic feature below or close to the tree line facilitates overgrowing and areas with fine-grained deposits (e.g., sand, debris) experienced faster overgrowing that boulder deposits (Fig. 7A). This explains why outwash fans and impact areas associated with major GLOFs capable to transport and deposit large boulders persist longer than those associated with minor GLOFs (Fig. 7A).

Various geomorphic processes were involved in reworking GLOF diagnostic features. Steep-sided inner slopes of breached dams were a subject to erosion and slope processes, while the evidence of pre-GLOF water levels (e.g., exposed fine-grained lake sediments, linear features associated with the abrasion of the lake shore) has been erased by water and wind erosion. The impact areas of GLOFs were frequently a subject of reworking by fluvial processes, bank erosion and meander shift. In rather exceptional cases, GLOF diagnostic features such as outwash fans and impact areas were overprinted by GLOF diagnostic features of latter, higher-magnitude GLOF. This is the example of Artizon / Santa Cruz valley in the Cordillera Blanca (see also Mergili et al., 2018). The first GLOF occurred in 1997 and left behind well-developed GLOF diagnostic features (outwash fan and impact area; see Fig. 8A,B). In 2012, the same area was impacted by another GLOF, overprinting still existing GLOF diagnostic features of the 1997 GLOF (Fig. 8C,D).

The anthropogenic activities can play specific but important role in degrading geomorphic GLOF diagnostic features. For instance, the geomorphic evidence of breached moraine dam of the lake Rajucolta (Cordillera Blanca) was erased in 2004 when the dam was remediated and equipped with artificial constructions. Another example of anthropogenic reworking of GLOF diagnostic features is the post-GLOF development of the impact area of the 1941 GLOF from the Lake Palcacocha in the Cordillera Blanca (Fig. 9A). Despite this notorious case in GLOF studies claimed at least 1800 fatalities in Huaraz, spontaneous development and spread of the city into the GLOF impact area have occurred in coming decades (see also Carey, 2010; Huggel et al., 2020). The part of the impact area near the confluence with the Rio Santa (area ≈ 0.7 km^2) has been gradually built-up and exhibits no evidence of GLOF impacts anymore (Fig. 9B).

Interesting insights are gained from the oldest GLOF in the inventory – the 1725 Rajururi GLOF which is documented to claim many lives in the Ancash village, Cordillera Blanca. While the magnitude of this event was likely extreme and the development of all GLOF diagnostic features is likely, no geomorphic evidence is found in the 1948 images, i.e., 223 years after the GLOF. Presumably, breached moraine dam was remodelled by advancing glaciers during the second phase of the Little Ice Age in the second half of 19th century (Thompson et al., 2000; Solomina et al., 2007), while outwash fan and impact area vanished as a result of a combination of succession of vegetation, fluvial and slope processes and anthropogenic activities. This case suggests the upper bound of the longevity of GLOF diagnostic features in the region and corroborates the assumption that most of the GLOFs in the recent GLOF inventory of Emmer et al. (2022b) are attributable to the post-LIA period.

3.3.2. Relative occurrence of degradation processes

Table 3 shows the occurrence of observed degradation processes in relation to individual types of GLOF diagnostic features. It is shown that the most frequently observed were the succession of vegetation (grass, shrubs, trees) over outwash fans (see example in Fig. 7 and impact areas (see the development in between Fig. 8B and Fig. 8C) and geomorphic reworking of impact areas (see the development between Fig. 8C and Fig. 8D). The succession of vegetation and geomorphic reworking were observed to degrade effectively all studied types of GLOF diagnostic features while anthropogenic activities only impacted breached dams by dam remediations and impact areas by agricultural cultivation and urban development (see examples in Section 3.3.1). The succession of vegetation exhibits gradual but often high change rate. The impact areas of some of the minor GLOFs were observed to be vanished within years (i.e., the reduction of identifiable impact area extent >10 % per year).

4. Discussion: implications for building GLOF inventories

4.1. Are we underestimating GLOF counts?

Emmer et al. (2022b) showed the imbalance among the major and minor GLOFs in the inventory through time. While major GLOFs have been occurring since the 1930s, minor GLOFs have been occurring since 1970s. Considering the results of this study, it is suggested that minor GLOFs occurred also before 1970s, but they were not recorded in documentary data sources and their geomorphic evidence vanished. Accepting this assumption, it can be approximated how many minor GLOFs remained undetected. Taking the sample of 89 dated GLOFs, 52 (58 %) are classified as major while the remaining 37 (42 %) are classified as minor. However, the ratio between minor and major GLOFs varies substantially in time (Fig. 10). While major GLOFs dominated in early decades, minor GLOFs have increased share in recent decades with

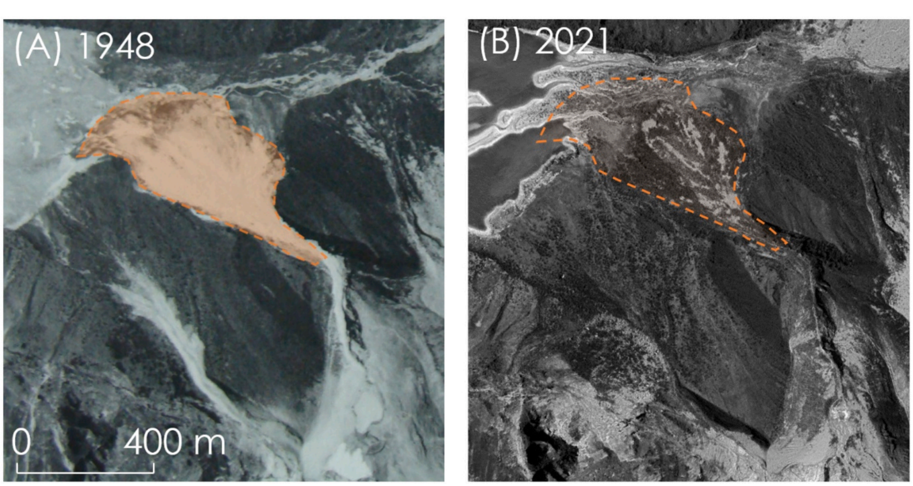

Fig. 7. An example of a degradation of GLOF diagnostic feature by the succession of vegetation. Part (A) shows the outwash fan (spatial extent highlighted in orange) associated with the 1945 Lake Chacrucocha GLOF in the C. Blanca in 1948, i.e., 3 years after the GLOF (aerial image: archive of the Autoridad Nacional del Agua, Huaraz, Peru); part (B) shows the same area in 2021, i.e., 76 years after the GLOF (satellite image: CNES / Airbus, 9th August 2021; available from the Google Earth Pro collection).

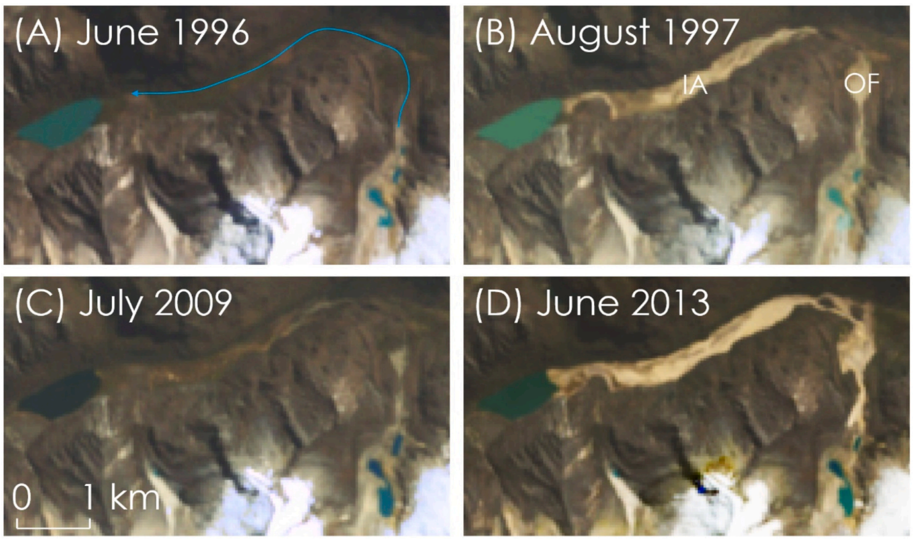

Fig. 8. An example of a degradation of GLOF diagnostic features by geomorphic reworking. Part (A) shows central part of the Santa Cruz valley with Artizon valley in June 1996, blue arrow indicates stream direction (image: Landsat, June 1996, available from the USGS LandsatLook collection); part (B) shows the same area in August 1997 (3 months after the GLOF) with clearly visible outwash fan (OF) and impact area (IA) (image: Landsat, August 1997; available from the USGS LandsatLook collection); part (C) shows the same area in July 2009; while the 1997 GLOF impact area has been largely overgrown by vegetation, outwash fan is still identifiable in the scene (image: Landsat, July 2009; available from the USGS LandsatLook collection); part (D) shows the same area affected by another GLOF in 2012 as seen in June 2013 (image: Landsat, June 2013; available from the USGS LandsatLook collection). Any remaining evidence of the 1997 GLOF has been overwritten by the larger 2012 GLOF in the landscape. (For interpretation of the references to colour in this figure legend, the reader is referred to the web version of this article.)

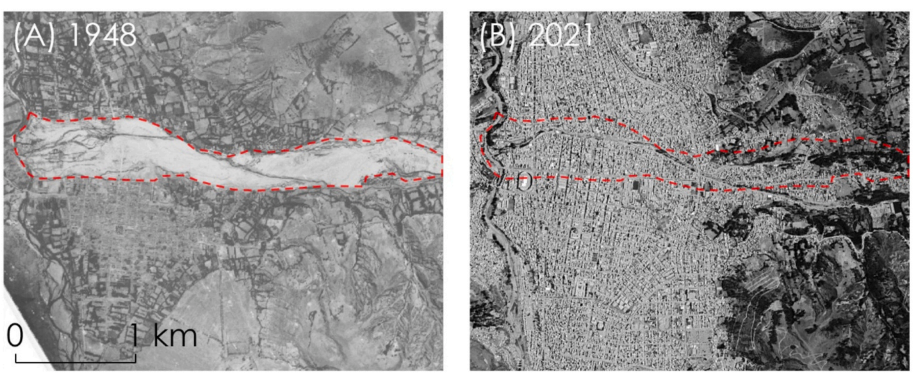

Fig. 9. An example of a degradation of GLOF diagnostic feature by anthropogenic activities. Part (A) shows part of the impact area (spatial extent highlighted by red dashed line) associated with the 1941 Lake Palcacocha GLOF in the C. Blanca as seen in 1948, i.e., 7 years after the GLOF (aerial image: archive of the Autoridad Nacional del Agua, Huaraz, Peru); part (B) shows the same area in 2021, i.e., 80 years after the GLOF, with superimposed 1941 GLOF impact area (satellite image: Maxar Technologies, 24th July 2021; available from the Google Earth Pro collection). (For interpretation of the references to colour in this figure legend, the reader is referred to the web version of this article.)

Table 3
The occurrence of various degradation processes for different types of GLOF diagnostic features (+ refers to rare occurrence (< 10 % of cases), + + refers to common occurrence (from 10 % to 25 % of cases), + + + refers to frequent occurrence (> 25 % of cases); – refers to no occurrence).

	Succession of vegetation	Geomorphic reworking	Anthropogenic activities
Breached dam	+ (grass, shrubs)	+ (slope processes, erosion, glacier re-advance)	+ (dam remediation)
Pre-GLOF water level	+ + (grass, shrubs)	+ + (slope processes, erosion, glacier re-advance)	–
Outwash fan	+ + + (grass, shrubs)	+ (fluvial processes, another GLOF)	–
GLOF impact area	+ + + (grass, shrubs, trees)	+ + + (fluvial and slope processes, another GLOF)	+ + (land cultivation, building-up floodplains)

69 % in 2011–2020. If 2011–2020 is considered reference period, and the number of minor GLOFs is calculated based on the number of major GLOFs, the expected total of GLOFs increases by 90 % compared to observation. If 2001–2020 is considered reference period, the expected total of GLOFs increases by 36 % compared to observations.

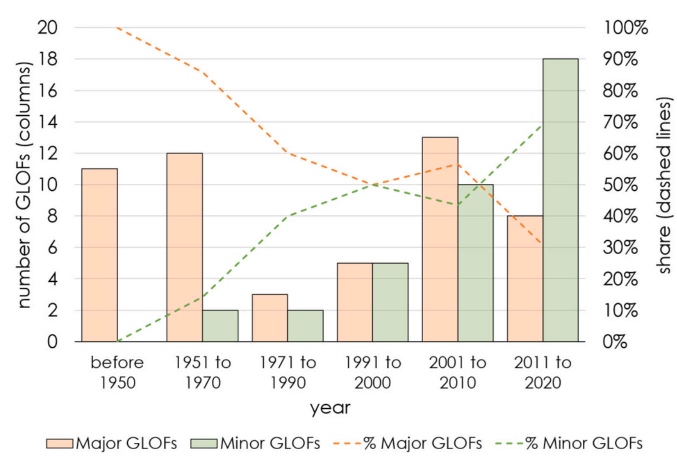

Fig. 10. The number and share of major and minor GLOFs in time (based on the 89 dated GLOFs).

Among the 71 not dated GLOFs, nineteen (37 %) are classified as major while remaining 52 (63 %) as minor. Considering all 160 GLOFs together (no matter whether dated or not), the is 71 major to 89 minor GLOFs. By applying expected proportional share of major and minor GLOFs derived from 2011 to 2020 reference period, it suggests that the GLOF total is underestimated by 44 %, while reference period 2001–2020 suggests that the GLOF total is underestimated by only 4 %.

Although this estimation is very rough and rather approximative, it gives a notion about the hiatus GLOF inventories might be facing and corresponds well with the lower bound of the estimation of Veh et al. (2022) who found out that two to four out of five GLOFs might have gone unnoticed in the pre-satellite era. Considering rather rich documentary data sources and well-developed GLOF inventory in the Andes of Peru and Bolivia, those estimates align well.

4.2. The role of lake dam types and GLOF mechanisms

The development of GLOF diagnostic features is influenced by glacial lake dam type (moraine-dammed, bedrock-dammed, ice-dammed, combined dams) and GLOF mechanisms (dam breach, dam overtopping) which in turn influence GLOF magnitude. For instance, the only plausible mechanism of GLOF from a bedrock-dammed lake is dam overtopping, because its bedrock dam is generally stable and – as a result – a breached dam cannot be developed in such a case. GLOFs originating from bedrock-dammed lakes are characterized by lower flood volumes and resulting faster flood attenuation compared to GLOFs originating from moraine dam failures. In the Emmer et al. (2022b) inventory used in this work, 76 % of major GLOFs are associated with moraine-dammed lakes while this number drops to 50 % in case of minor GLOFs, partly explaining differences in developed GLOF diagnostic features (Fig. 5). On the other hand, minor GLOFs originated from lakes with combined dams in 30 % while major GLOFs in <10 % cases (Emmer et al., 2022b).

In the study focusing on the Peruvian Cordillera Blanca, Emmer et al. (2020) observed increased share of GLOFs from bedrock-dammed lakes in recent decades. Apart from observed shift from moraine- to bedrock-dammed lakes among the proglacial lakes, this increased share can also be (partly) explained by various GLOF mitigation measures implemented especially to moraine-dammed lakes (e.g., Reynolds, 1992; Portocarrero, 2014; Emmer et al., 2018) and/or weaker geomorphic evidence of GLOFs originating from bedrock-dammed lakes. Glacial lake outburst floods from bedrock-dammed lakes are typically associated with outwash fans and impact areas – the least persistent GLOF diagnostic features. At the same time, dam overtopping is less likely to generate major GLOF (Emmer et al., 2022b). For these reasons, minor GLOFs from bedrock-dammed lakes are especially likely to be missed in remote sensing image analysis-based GLOF inventories.

5. Conclusions

Glacial lake outburst floods are assuredly characterized by their capability to produce long-persistent geomorphic imprints. Building on the observations from the Andes of Peru and Bolivia, this study presents the first attempt to quantify how long are different types of GLOF diagnostic features (expected to be) preserved in the landscape. This question is of special importance for building GLOF inventories and estimating the number of possibly missed GLOFs, especially in the pre-satellite period. A total of 359 GLOF diagnostic features associated with 156 GLOFs are analyzed in this work, revealing their relative occurrence among different GLOF magnitudes, mechanisms and lake dam types involved. Further, degradation processes responsible for vanishing GLOF diagnostic features are analyzed. It is shown that especially breached dams are long-lasting GLOF diagnostic features unlikely to vanish in the post-LIA timeframe while outwash fans and impact areas may vanish within decades, even in the case of a major, far-reaching GLOF. As such, the geomorphic evidence of GLOFs associated with moraine dam breaches is considered stable in given temporal context. This assumption allowed to estimate the number of possibly missed GLOFs in the inventory, using the number of major GLOFs as a predictor of the number of minor GLOFs. It is concluded that up to 40 % of GLOFs (especially minor GLOFs originating from bedrock-dammed lakes) may be missing in the record, if 2011–2020 is taken as the reference period. This estimation is in line with the lower bound of the global GLOF reporting hiatus estimation of Veh et al. (2022). However, considering specific climatic and environmental conditions of the study area (and so possibly specific types and intensity of degradation processes and longevity of GLOF diagnostic features), these findings may not be directly transferred to different geographical contexts without essentially analyzing the specific factors of the longevity of GLOF diagnostic features there, which I call for. The integration of various data sources and especially the exploitation of existing sets of archival aerial photographs in combination with satellite products with increasing spatial and temporal resolution are recommended to tackle this challenging task of quantifying possible biases that are associated with vanishing GLOF evidence in existing GLOF inventories.

Declaration of competing interest

The authors declare that they have no known competing financial interests or personal relationships that could have appeared to influence the work reported in this paper.

Data availability

Data will be made available on request.

Acknowledgement

The author would like to thank two anonymous reviewers for their helpful comments and suggestions. Further, Ing. Alejo Cochachin – the head of the glaciology unit of the Autoridad Nacional del Agua (ANA) - is thanked for granting the access to the ANA archive in Huaraz, Peru. The author is a member of the RCUK-CONCYTEC Glacial Lakes of Peru (GLOP) project. This research has not received any specific project funding. The financial support by the University of Graz is acknowledged for funding the open access of this publication.

References

Abdel-Fattah, D., Trainor, S., Hood, E., Hock, R., Kienholz, C., 2021. User engagement in developing use-inspired glacial lake outburst flood decision support tools in Juneau and the Kenai Peninsula, Alaska. Front. Earth Sci. 9, 635163 https://doi.org/10.3389/feart.2021.635163.

Bat'ka, J., Vilímek, V., Štefanová, E., Cook, S.J., Emmer, A., 2020. Glacial Lake Outburst Floods (GLOFs) in the Cordillera Huayhuash, Peru: historic events and current susceptibility. Water 12, 2664. https://doi.org/10.3390/w12102664.

Carey, M.P., 2010. In the Shadow of Melting Glaciers: Climate Change And Andean Society. Oxford University Press, New York, USA.

Carrivick, J.L., Tweed, F.S., 2016. A global assessment of the societal impacts of glacier outburst floods. Glob. Planet. Chang. 144, 1–16. https://doi.org/10.1016/j.gloplacha.2016.07.001.

Carrivick, J.L., Tweed, F.S., 2019. A review of glacier outburst floods in Iceland and Greenland with a megafloods perspective. Earth-Sci. Rev. 196, 102876 https://doi.org/10.1016/j.earscirev.2019.102876.

Carrivick, J.L., Tweed, F.S., Ng, F., Quincey, D.J., Mallalieu, J., Ingeman-Nielsen, T., Mikkelsen, A.B., Palmer, S.J., Yde, J.C., Homer, R., Russell, A.J., Hubbard, A., 2017. Ice-dammed lake drainage evolution at Russell Glacier, West Greenland. Front. Earth Sci. 5, 100. https://doi.org/10.3389/feart.2017.00100.

Emmer, A., 2017. Geomorphologically effective floods from moraine-dammed lakes in the Cordillera Blanca,Peru. Quat. Sci. Rev. 177, 220–234. https://doi.org/10.1016/j.quascirev.2017.10.028.

Emmer, A., Vilímek, V., Huggel, C., Klimeš, J., Schaub, Y., 2016. Limits and challenges to compiling and developing a database of glacial lake outburst floods. Landslides 13, 1579–1584. https://doi.org/10.1007/s10346-016-0686-6.

Emmer, A., Vilímek, V., Zapata, M.L., 2018. Hazard mitigation of glacial lake outburst floods in the Cordillera Blanca (Peru): the effectiveness of remedial works. J.Flood Risk Manag. 11 (S1), 489–501.

Emmer, A., Harrison, S., Mergili, M., Allen, S., Frey, H., Huggel, C., 2020. 70 years of lake evolution and glacial lake outburst floods in the Cordillera Blanca (Peru) and implications for the future. Geomorphology 365, 107178. https://doi.org/10.1016/j.geomorph.2020.107178.

Emmer, A., Allen, S.K., Carey, M., Frey, H., Huggel, C., Korup, O., Mergili, M., Sattar, A., Veh, G., Chen, T.Y., Cook, S.J., Correas-Gonzalez, M., Das, S., Diaz Moreno, A., Drenkhan, F., Fischer, M., Immerzeel, W.W., Izagirre, E., Joshi, R.C., Kougkoulos, I., Kuyakanon Knapp, R., Li, D., Majeed, U., Matti, S., Moulton, H., Nick, F., Piroton, V., Rashid, I., Reza, M., Ribeiro de Figueiredo, A., Riveros, C., Shrestha, F., Shrestha, M., Steiner, J., Walker-Crawford, N., Wood, J.L., Yde, J.C., 2022a. Progress and challenges in glacial lake outburst flood research (2017–2021): a research

community perspective. Nat. Hazards Earth Syst. Sci. 22, 3041–3061. https://doi.org/10.5194/nhess-22-3041-2022.
Emmer, A., Wood, J.L., Cook, S.J., Harrison, S., Wilson, R., Diaz-Moreno, A., Reynolds, J. M., Torres, J.C., Yarleque, C., Mergili, M., Jara, H.W., Bennett, G., Caballero, A., Glasser, N.F., Melgarejo, E., Riveros, C., Shannon, S., Turpo, E., Tinoco, T., Torres, L., Garay, D., Villafane, H., Garrido, H., Martinez, C., Apaza, N., Araujo, J., Poma, C., 2022b. 160 Glacial lake outburst floods (GLOFs) across the Tropical Andes since the Little Ice Age. Glob. Planet. Chang. 208, 103722 https://doi.org/10.1016/j.gloplacha.2021.103722.
Field, H.R., Armstrong, W.H., Huss, M., 2021. Gulf of Alaska ice-marginal lake area change over the Landsat record and potential physical controls. Cryosphere 15, 3255–3278. https://doi.org/10.5194/tc-15-3255-2021.
Haeberli, W., Drenkhan, F., 2022. Future lake development in deglaciating mountain ranges. In: Cutter, L.S. (Ed.), Oxford Research Encyclopedias – Natural Hazard Science. Oxford University Press, pp. 1–45. https://doi.org/10.1093/acrefore/9780199389407.013.361.
Harrison, S., Kargel, J.S., Huggel, C., Reynolds, J., Shugar, D.H., Betts, R.A., Emmer, A., Glasser, N., Haritashya, U.K., Klimeš, J., Reinhardt, L., Schaub, Y., Wiltshire, A., Regmi, D., Vilímek, V., 2018. Climate change and the global pattern of moraine-dammed glacial lake outburst floods. Cryosphere 12, 1195–1209. https://doi.org/10.5194/tc-12-1195-2018.
Huggel, C., Carey, M., Emmer, A., Frey, H., Walker-Crawford, N., Wallimann-Helmer, I., 2020a. Anthropogenic climate change and glacier lake outburst flood risk: local and global drivers and responsibilities for the case of lake Palcacocha, Peru. Nat. Hazard Earth Syst. Sci. 20, 2175–2193. https://doi.org/10.5194/nhess20-2175-2020.
Ikeda, N., Narama, C., Gyalson, S., 2016. Knowledge sharing for disaster risk reduction: insights from a glacier lake workshop in the Ladakh RegionIndian Himalayas. Mt. Res. Dev. 36 (1), 31–40. https://doi.org/10.1659/MRD-JOURNAL-D-15-00035.1.
INAIGEM, 2018. El inventario nacional de glaciares: las cordilleras glaciares del Perú. Instituto Nacional de Investigación en Glaciares y Ecosistemas de Montaña (INAIGEM), Lima (Peru).
Jacquet, J., McCoy, S.W., McGrath, D., Nimick, D.A., Fahey, M., O'Kuinghttons, J., Friesen, B.A., Leidich, J., 2017. Hydrologic and geomorphic changes resulting from episodic glacial lake outburst floods: Rio Colonia, Patagonia, Chile. Geophys. Res. Lett. 44, 854–864. https://doi.org/10.1002/2016GL071374.
Jomelli, V., Grancher, D., Brunstein, D., Solomina, O., 2008. Recalibration of the yellow Rhizocarpon growth curve in Cordillera Blanca (Peru) and implications for LIA chronology. Geomorphology 93, 201–212. https://doi.org/10.1016/j.geomorph.2007.02.021.
Kirschbaum, D., Watson, C.S., Rounce, D.R., Shugar, D.H., Kargel, J.S., Haritashya, U.K., Amatya, P., Shean, D., Anderson, E.R., Jo, M., 2019. The state of remote sensing capabilities of cascading hazards over high mountain Asia. Front. Earth Sci. 7, 197. https://doi.org/10.3389/feart.2019.00197.
Maurer, J.M., Schaefer, J.M., Russell, J.B., Rupper, S., Wangdi, N., Putnam, A.E., Young, N., 2020. Seismic observations, numerical modeling, and geomorphic analysis of a glacier lake outburst flood in the Himalayas. Sci. Adv. 6, eaav3645 https://doi.org/10.1126/sciadv.aba3645.
Mergili, M., Emmer, A., Juřicová, A., Cochachin, A., Fischer, J.-T., Huggel, C., Pudasaini, S.P., 2018. How well can we simulate complex hydro-geomorphic process chains? The 2012 multi-lake outburst flood in the Santa Cruz Valley (Cordillera Blanca, Perú). Earth Surf. Proc. Land. 43, 1373–1389. https://doi.org/10.1002/esp.4318.
Monegato, G., Mozzi, P., Paiero, G., Rossato, S., 2020. Sedimentary evidence of glacial lake outburst floods (GLOFs) during the last glacial maximum in the Venetian-Friulian plain (NE Italy). Quat. Int. 538, 44–52. https://doi.org/10.1016/j.quaint.2018.04.042.
Motschmann, A., Huggel, C., Muñoz, R., Thür, A., 2020. Towards integrated assessments of water risks in deglaciating mountain areas: water scarcity and GLOF risk in the Peruvian Andes. Geoenviron. Dis. 7, 1–18. https://doi.org/10.1186/s40677-020-00159-7.
Nie, Y., Liu, Q., Wang, J., Zhang, Y., Sheng, Y., Liu, S., 2018. An inventory of historical glacial lake outburst floods in the Himalayas based on remote sensing observations and geomorphological analysis. Geomorphology 308, 91–106. https://doi.org/10.1016/j.geomorph.2018.02.002.
Piret, L., Bertrand, S., Nguyen, N., Hawkings, J., Rodrigo, C., Wadham, J., 2022. Long-lasting impacts of a 20th century glacial lake outburst flood on a Patagonian fjord-river system (Pascua River). Geomorphology 399, 108080. https://doi.org/10.1016/j.geomorph.2021.108080.
Portocarrero, C.A., 2014. Reducing the Risk of Dangerous Lakes in the Peruvian Andes: A Handbook for Glacial Lake Management. US Agency for International Development, Washington, 68 pp.
Rabatel, A., Francou, B., Soruco, A., Gomez, J., Cáceres, B., Ceballos, J.L., Basantes, R., Vuille, M., Sicart, J.-E., Huggel, C., Scheel, M., Lejeune, Y., Arnaud, Y., Collet, M., Condom, T., Consoli, G., Favier, V., Jomelli, V., Galarraga, R., Ginot, P., Maisincho, L., Mendoza, J., Ménégoz, M., Ramirez, E., Ribstein, P., Suarez, W., Villacis, M., Wagnon, P., 2013. Current state of glaciers in the tropical Andes: a multi-century perspective on glacier evolution and climate change. Cryosphere 7, 81–102. https://doi.org/10.5194/tc-7-81-2013.
Reynolds, J.M., 1992. The identification and mitigation of glacier-related hazards: examples from the Cordillera Blanca, Peru. In: McCall, G.J.H., Laming, D.C.J., Scott, S. (Eds.), Geohazards. Chapman & Hall, London, pp. 143–157.
Richard, D., Gay, M., 2004. Survey and Prevention of Extreme Glaciological Hazards in European Mountainous Regions. Final Report, Glaciorisk Project, FP5.
Rothe, T.O., Bakke, J., Storen, E.W.N., 2019. Glacier outburst floods reconstructed from lake sediments and their implications for Holocene variations of the plateau glacier Folgefonna in western Norway. Boreas 48 (3), 616–634. https://doi.org/10.1111/bor.12388.
Solomina, O., Jomelli, V., Kaser, G., Ames, A., Berger, B., Pouyaud, B., 2007. Lichenometry in the Cordillera Blanca, Peru: "Little Ice Age" moraine chronology. Glob. Planet. Chang. 59 (1–4), 225–235.
Taylor, L.S., Quincey, D.J., Smith, M.W., Baumhoer, C.A., McMillian, M., Mansell, D.T., 2021. Remote sensing of the mountain cryosphere: current capabilities and future opportunities for research. Prog.Phys.Geogr.EarthEnviron. 45, 931–964. https://doi.org/10.1177/03091333211023690.
Thompson, L., Mosley-Thompson, E., Henderson, K., 2000. Ice-core paleoclimate records in tropical South America since the last glacial maximum. J. Quat. Sci. 15, 107–115.
Tomczyk, A.M., Ewertowski, M.W., Carrivick, J.L., 2020. Geomorphological impacts of a glacier lake outburst flood in the high arctic Zackenberg River, NE Greenland. J. Hydrol. 591, 125300 https://doi.org/10.1016/j.jhydrol.2020.125300.
Vandekerkhove, E., Bertrand, S., Torrejon, F., Kylander, M.E., Reid, B., Saunders, K.M., 2021. Signature of modern glacial lake outburst floods in fjord sediments (Baker River, southern Chile). Sedimentology 68, 2798–2819. https://doi.org/10.1111/sed.12874.
Veh, G., Korup, O., Roessner, S., Walz, A., 2018. Detecting Himalayan glacial lake outburst floods from Landsat time series. Remote Sens. Environ. 207, 84–97. https://doi.org/10.1016/j.rse.2017.12.025.
Veh, G., Korup, O., von Specht, S., Roessner, S., Walz, A., 2019. Unchanged frequency of moraine-dammed glacial lake outburst floods in the Himalaya. Nat. Clim. Chang. 9, 379–383. https://doi.org/10.1038/s41558-019-0437-5.
Veh, G., Lützov, N., Kharlamova, V., Petrakov, D., Hugonnet, R., Korup, O., 2022. Trends, breaks, and biases in the frequency of reported glacier lake outburst floods. Earth's Future 10, e2021EF002426. https://doi.org/10.1029/2021EF002426.
Vilca, O., Mergili, M., Emmer, A., Frey, H., Huggel, C., 2021. The 2020 glacial Lake outburst flood process chain at Lake Salkantaycocha (Cordillera Vilcabamba, Peru). Landslides 18, 2211–2223. https://doi.org/10.1007/s10346-021-01670-0.
Vilímek, V., Emmer, A., Huggel, C., Schaub, Y., Würmli, S., 2014. Database of glacial lake outburst floods (GLOFs) – IPL Project No. 179. Landslides 11, 161–165. https://doi.org/10.1007/s10346-013-0448-7.
Wang, S.J., Zhou, L.Y., 2017. Glacial lake outburst flood disasters and integrated risk management in China. Int.J.Disaster Risk Sci. 8 (4), 493–497. https://doi.org/10.1007/s13753-017-0152-7.
Wang, X., Guo, X., Yang, C., Liu, Q., Wei, J., Zhang, Y., Liu, S., Zhang, Y., Jiang, Z., Tang, Z., 2020. Glacial lake inventory of high-mountain Asia in 1990 and 2018 derived from Landsat images. Earth Syst. Sci. Data 12, 2169–2182. https://doi.org/10.5194/essd-12-2169-2020.
Zheng, G., Bao, A., Allen, S., Ballesteros-Canovas, J.A., Yuan, Y., Jiapaer, G., Stoffel, M., 2021. Numerous unreported glacial lake outburst floods in the Third Pole revealed by high-resolution satellite data and geomorphological evidence. Sci. Bull. 66, 1270–1273. https://doi.org/10.1016/j.scib.2021.01.014.

Data / databases / online repositories

Google Earth Pro collection. Available from URL: <https://www.google.com/intl/cs/earth/versions/>; last accessed (September 2022).
USGS EarthExplorer, United States Geological Survey Earth Explorer. Available from URL: <https://earthexplorer.usgs.gov>; last accessed (September 2022).
USGS LandsatLook, United States Geological Survey LandsatLook. Available from URL: https://landsatlook.usgs.gov>; last accessed (September 2022).
Sentinel EO browser. Available from URL: <https://apps.sentinel-hub.com/eo-browser/>; last accessed (September 2022).